

Firing properties and functional connectivity of substantia nigra pars compacta neurones recorded with a multi-electrode array *in vitro*

Nicola Berretta¹, Giorgio Bernardi^{1,2} and Nicola B. Mercuri^{1,2}

¹Fondazione Santa Lucia IRCCS, Rome, Italy

²Clinica Neurologica, University of Rome 'Tor Vergata', Rome, Italy

Dopamine (DA) neurones of the substantia nigra pars compacta (SNc) are involved in a wide variety of functions, including motor control and reward-based learning. In order to gain new insights into the firing properties of neuronal ensembles in the SNc, we recorded extracellular single units from spontaneously active neurones, using a multi-electrode array (MEA) device in midbrain slices. The majority of neurones (50.21%) had a low firing frequency (1–3 Hz) and a stable pacemaker-like pattern, while others (44.84%) were irregular, but still firing at a low rate. The remaining population (4.95%) comprised neurones with a regular higher firing rate (5–10 Hz). High rate neurones, on the whole, were insensitive to DA (30 μ M), while low rate neurones were mostly inhibited by DA, although responding either with a prominent or a weak inhibition. However, we recorded low rate regular neurones that were insensitive to DA, or irregular low rate neurones excited by DA. Interestingly, we found pairs of active neurones (12.10 \pm 3.14%) with a significant proportion of spikes occurring synchronously. Moreover, the crosscorrelation probability in each pair tended to increase in response to DA. In conclusion, MEA recordings in midbrain slices reveal a much more complex picture than previously reported with regard to the firing pattern and DA sensitivity of spontaneously active SNc neurones. Moreover, the study opens new perspectives for the *in vitro* investigation of functional connectivity in the midbrain dopaminergic system, thus proposing new targets for the pharmacological treatment of DA-dependent neurological disorders.

(Resubmitted 1 March 2010; accepted after revision 23 March 2010; first published online 29 March 2010)

Corresponding author N. Berretta: Fondazione Santa Lucia IRCCS – Via del Fosso di Fiorano 64, 00143 Rome, Italy.

Email: n.berretta@hsantalucia.it

Abbreviations CV, coefficient of variation; DA, dopamine; HR, high rate; I_h , hyperpolarisation-activated cationic current; LR, low rate; LRn-p, non-pacemaker low rate; LRP, pacemaker low rate; MEA, multi-electrode array; MT, medial terminal nucleus of the accessory optic tract; SNc, substantia nigra pars compacta; VTA, ventral tegmental area.

Introduction

Substantia nigra pars compacta (SNc) neurones have attracted much interest in neuroscience since the early 1980s for their involvement in motor control and reward-based learning, in addition to extrapyramidal movement disorders such as Parkinson's disease (Grace & Bunney, 1983a; Björklund & Dunnett, 2007; Schultz, 2007; Wise, 2009). It is well established that the SNc contains dopamine (DA)-releasing neurones, thus called DA neurones, electrophysiologically characterised by a broad action potential, a hyperpolarisation-activated cationic current (I_h), regular 1–5 Hz pacemaker-like firing in *in vitro* conditions, and a DA-mediated membrane hyperpolarisation, through stimulation of D2 autoreceptors

(Lacey *et al.* 1987, 1989; Grace & Onn, 1989; Mercuri *et al.* 1995; Beckstead *et al.* 2004). In addition, the SNc contains non-DA neurones, representing a local population of inhibitory, γ -amino-butyric acid (GABA)-releasing, interneurones, characterised by a higher firing rate (\sim 10 Hz) and insensitivity to DA (Lacey *et al.* 1989; Grace & Onn, 1989). This distinction, though generally accepted for the SNc, has been recently questioned for the nearby ventral tegmental area (VTA), in which the immunohistochemical characterisation of the DA neurones has been shown to be somewhat unrelated to their membrane properties and DA sensitivity (Margolis *et al.* 2006; Lammel *et al.* 2008).

The last decade has seen a growing interest in the electrophysiological investigation of neuronal ensembles *in vitro* using multi-electrode array (MEA) technology

(Egert *et al.* 1998; Oka *et al.* 1999; Stett *et al.* 2003; Whitson *et al.* 2006), or optical recordings (Takahashi *et al.* 2007), thus opening new frontiers in network neurophysiology. MEA recordings, in particular, have been mostly applied to describe the spatio-temporal dynamics of neuronal oscillations and of synaptic field responses (Mann *et al.* 2005; Mapelli & D'Angelo, 2007; van Aerde *et al.* 2008). However, MEAs may also be used for single-unit action potential recordings from acute slice preparations (Egert *et al.* 2002; Geracitano *et al.* 2005; Giustizieri *et al.* 2007; Jia *et al.* 2008; Kent & Meredith, 2008), allowing the simultaneous detection of spikes arising from a large population of different cell types, responding differently to treatments. Indeed, MEA recordings of neuronal firing may represent a new approach for the investigation of spontaneously active neurones of the SNc, providing new insights into the firing properties of its neuronal populations, in controlled and non-invasive experimental conditions, with regard to the relationship between cell and recording electrode.

Moreover, recent evidence demonstrates that the DA neurones of the SNc may act in a synchronised manner, especially in response to rewarding events (Morris *et al.* 2004; Joshua *et al.* 2009). An *in vitro* investigation of the functional connectivity among the DA neurones certainly requires a MEA approach, particularly because the number of pairs of DA neurones appears to be limited (Morris *et al.* 2004), thus a large amount of experimental data is required from the same preparation.

In previous experiments we have shown that the MEA technique can be successfully used in the analysis of the collective responses of SNc neurones to specific treatments (Geracitano *et al.* 2005; Giustizieri *et al.* 2007). In the present work we provide a general description of the neuronal populations recorded in the SNc with this technique, demonstrating a much more complex picture than previously reported with regard to their firing pattern and DA sensitivity. Moreover, we present evidence of neuronal synchronisation, hence proposing new areas for investigation of the dopaminergic system *in vitro*.

Methods

Slice preparation

Wistar rats (28–40 days old) were anaesthetised with halothane and killed by decapitation. All experiments followed international guidelines on the ethical use of animals from the European Communities Council Directive of 24 November 1986 (86/609/EEC). The brain was removed from the skull and horizontal midbrain slices (300 μm) were cut in cold (8–12°C) artificial cerebrospinal fluid (ACSF) and left to recover at 34°C for at least one hour. ACSF composition was the following (in mM): NaCl

126; KCl 2.5; MgCl_2 1.3; CaCl_2 2.4; NaH_2PO_4 1.2; NaHCO_3 24; glucose 10; saturated with 95% O_2 , 5% CO_2 (pH 7.4).

Multi-electrode array recordings

Individual slices were placed over an 8×8 array of planar microelectrodes, each $20 \mu\text{m} \times 20 \mu\text{m}$ in size, with an interpolar distance of 100 μm (MED-P2105; Alpha MED Sciences, Kadoma, Japan). Slices were positioned over the multi-electrode array under visual control through an upright microscope (Leica DM-LFS, Leica Microsystems, Wetzlar, Germany), so that most of the planar electrodes were covered by the SNc area. The location of the medial terminal nucleus of the accessory optic tract (MT) was taken as a reference for the SNc area (bregma -8.42 to -7.80 mm; Paxinos & Watson, 1986) and electrodes were never positioned medially to the MT, in order to avoid contamination from VTA (Fig. 1Aa). In a subset of control experiments, recordings were obtained from coronal mid-brain slices. In these experiments the SNc was identified as the elongated area located immediately lateral to the MT or the medial lemniscus (bregma -5.20 to -6.04 mm; Paxinos & Watson, 1986). Voltage signals were acquired using the MED64 System (Alpha MED Sciences), digitized at 20 kHz and filtered (0.1–10 kHz) with a 6071E Data Acquisition Card (National Instruments, Austin, USA), using Conductor software (Alpha MED Sciences).

The slices were kept submerged in ACSF with a nylon mesh glued to a platinum ring. Particular care was required to maintain a continuous flow of warm (34°C) oxygenated ACSF (4 ml min^{-1}), streaming right above the SNc area. This procedure allowed us to preserve the stable spontaneous firing of the neuronal population recorded.

Data acquisition and analysis

The fast transients corresponding to spontaneous action potentials were captured off-line using Spike2 6.0 software (Cambridge Electronic Design Ltd, Cambridge, UK), by means of an amplitude threshold adjusted by visual inspection in each individual active channel. Spikes could differ in shape and amplitude, reflecting spontaneous action potentials arising from more than one neurone, therefore spike-sorting discrimination of multi-unit responses was achieved by generating spike templates with Spike2 6.0, sorted with a normal mixtures algorithm on independent clusters obtained from principal component data (Fig. 1B).

Time stamps from neuronal data were analysed with NeuroExplorer software (Nex Technologies, Littleton, MA, USA). Separate units were characterised according to their firing rate, firing regularity and spike synchrony. The firing rate was measured both in control and during the time when a steady-state level of DA effect had been

achieved. The coefficient of variation (CV) was calculated by dividing the standard deviation of the inter-spike interval (ISI) by the mean ISI, during control. Spike time autocorrelation probability histograms were constructed for spikes recorded in control conditions, with a 10 ms bin size, and smoothed with a width 3 boxcar filter. The degree of regularity was assessed by the peak value of the histogram, and by the number of symmetric consecutive peaks exceeding the 99% confidence limit, measured according to the method defined by Abeles (1982). In order to evaluate the degree of autocorrelation during the whole time of recording, autocorrelation *vs.* time plots were constructed by measuring the autocorrelation probability in consecutive 10 s intervals, using the same binning and smoothing parameters mentioned above. Autocorrelation probability was then expressed by a colorimetric scale.

Spike synchrony was analysed by constructing cross-correlation histograms (± 500 ms, 1 ms bin size) between each of the simultaneously recorded units, smoothed with a width 3 boxcar filter, calculated over the whole time of recording (7–9 min). A pair of neurones was considered synchronous if there was a clear peak exceeding the 99% confidence limit, assessed according to the method described by Abeles (1982). Crosscorrelation *vs.* time diagrams were constructed (± 10 ms, 1 ms bin size, width 3 boxcar filter) in 10 s consecutive shifts, with crosscorrelation probability expressed by a colorimetric scale. In those cells in which synchronous firing was detected, according to the above-mentioned criteria, further analysis was conducted in order to evaluate if firing synchrony was affected by DA. For this analysis, the crosscorrelation probability (± 10 ms, 1 ms bin size, width 3 boxcar filter) was measured during 1 min control, immediately prior to DA perfusion, and 1 min in DA, or as soon as spikes recovered during DA washout.

Summary data are expressed as mean \pm S.E.M. Two-tailed Student's *t* test for paired or unpaired data, with $P < 0.05$ as the minimum level for statistical significance, was used.

Drugs

Dopamine hydrochloride (DA; Sigma-Aldrich, Milan, Italy) was dissolved in ASCF immediately before every experimental session and bath applied.

Results

Spontaneous spikes from 950 cells were recorded from 15 horizontal slices of the ventral midbrain. A single slice was positioned in a MEA recording chamber in such a way that most of the 64 planar electrodes covered the SNC area, identified as the crescent region around the dark spot corresponding to the MT (Fig. 1Aa; Paxinos & Watson,

1986). In order to limit the possible contamination from VTA neurones, the electrode array was never positioned medially to the MT. Spontaneous firing was evident in many of the 64 channels as negative and/or positive fast deflections above the noise level (Fig. 1B), which were completely abolished by tetrodotoxin ($1 \mu\text{M}$; not shown). On average, we recorded spikes from 30.47 ± 1.63 channels per slice. A single active channel could detect activity from one or multiple units sorted off-line (Fig. 1B; see Methods). Therefore, on average, we recorded spontaneous spikes arising from 63.34 ± 6.27 cells per slice.

We then proceeded into a classification of the neuronal population recorded. A criterion often used to discriminate neurones using extracellular single-unit spike recordings is the action potential waveform. However, in our experimental conditions, electrode position in relation to the recorded neurone could not be controlled. Thus, action potential shape was highly variable, according to the distance between electrode and site of action potential generation, or to whether spikes from proximal dendrites rather than from the soma had been detected. In fact, as we will show later (Fig. 8), the same neurone could give rise to extracellular spikes with opposite polarity. For this reason, we considered the firing properties as the sole criterion to discriminate local neuronal populations.

Characterisation of the neuronal populations

The great majority of the neurones recorded were characterised by a pacemaker-like firing, whose regularity could be emphasised by the presence of multiple equally spaced peaks in their spike time autocorrelograms (Fig. 2). We separated neuronal populations according to their basal firing frequency and to the regularity in their firing, assessed by the number of symmetric peaks of their autocorrelograms, exceeding the 99% confidence limit (Abeles, 1982). We first identified a 'high rate' (HR) and a 'low rate' (LR) neuronal population, by selecting neurones with a basal firing rate above or below 4.5 Hz, respectively. HR neurones (Fig. 2Aa; Table 1) represented a relatively small proportion of the whole neuronal population recorded ($n = 47$; 4.95%). They had a mean basal firing frequency of 7.85 ± 0.51 Hz and were characterised by a regular pacemaker-like firing pattern, as indicated by the number of significant repetitive peaks in the spike time autocorrelation (6.60 ± 0.66), the autocorrelation probability measured on the first of the repetitive peaks ($18.27 \pm 0.91\%$) and their CV (0.49 ± 0.03). Conversely, the firing pattern of the LR neurones was not uniform, therefore this population was further subdivided according to the regularity of firing, using a criterion analogous to that used in *in vivo* investigations, based on the presence of significant

consecutive peaks in the spike time autocorrelogram (Tepper *et al.* 1995; Brazhnik *et al.* 2008). We defined *pacemaker* low rate (LRp) neurones as those LR cells with the number of significant peaks in the spike time autocorrelogram higher than 3, while *non-pacemaker* low rate (LRn-p) neurones were LR cells with 0–3 autocorrelation peaks. LRp neurones (Fig. 2*Ab*; Table 1) constituted 50.21% ($n = 477$) of all the recorded neurones. They had a mean basal firing frequency of 2.27 ± 0.03 Hz and highly regular firing, an autocorrelation probability

of $15.40 \pm 0.28\%$, measured on the first of the repetitive peaks and a CV of 0.46 ± 0.01 . Conversely, LRn-p neurones (Fig. 2*Ac*; Table 1) constituted 44.84% ($n = 426$) of the recorded neurones and their firing (1.19 ± 0.04 Hz) was irregular with a first peak spike autocorrelation probability of $5.71 \pm 0.13\%$ and a CV of 0.72 ± 0.02 .

The appropriateness of the criteria used in the subdivision of the entire population into HR, LRp and LRn-p neurones found an indirect validation when we looked at the distribution of their basal firing frequency

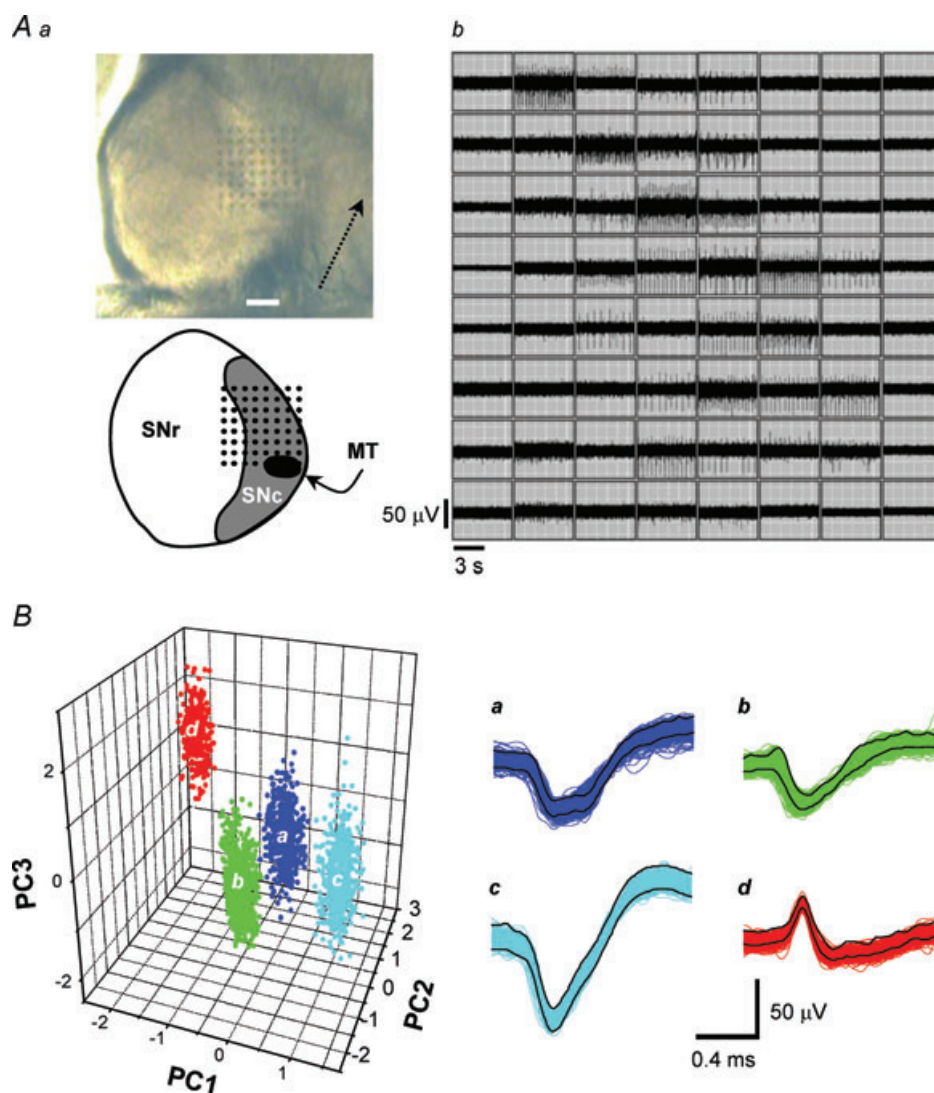
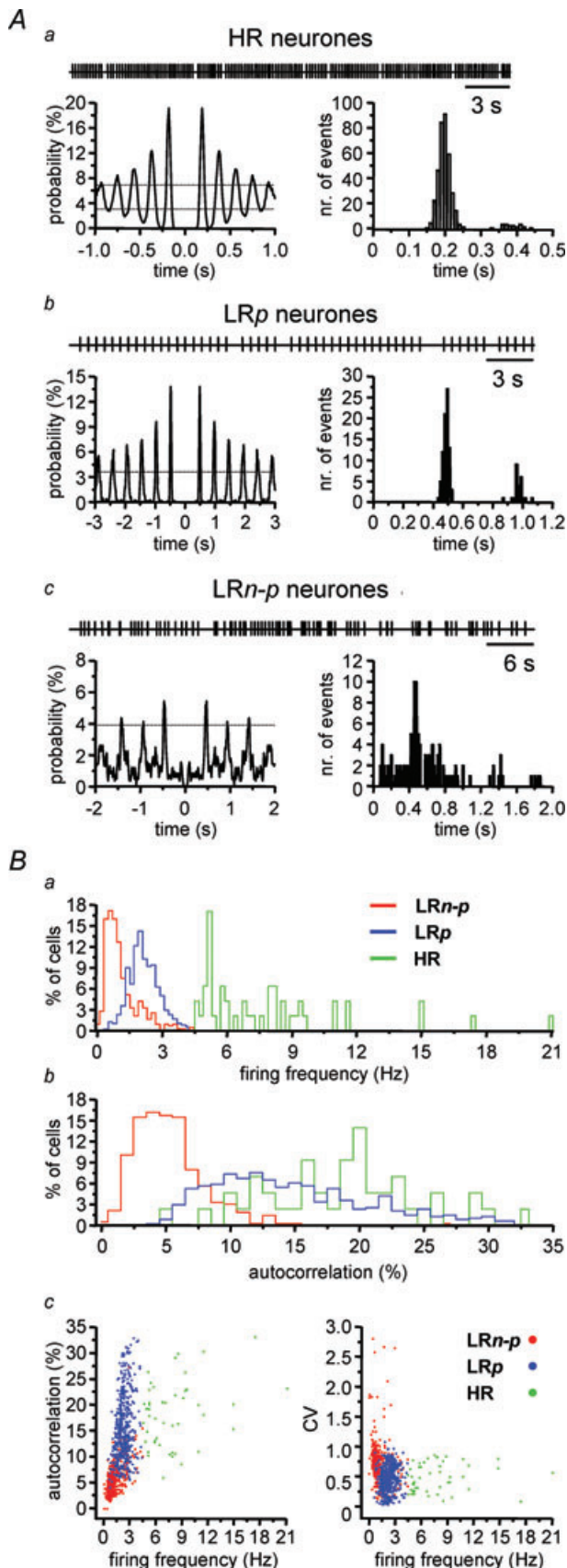


Figure 1. MEA recordings from a horizontal midbrain slice

Aa, photograph of a midbrain slice placed over an array of planar multi-electrodes, detectable in transparency through the slice. The schematic drawing below highlights electrode position in relation to substantia nigra pars compacta (SNc), the substantia nigra pars reticulata (SNr) and the medial terminal nucleus of the accessory optic tract (MT). The dotted arrow is placed medially to the SNc and points towards the frontal direction, along the fronto-caudal axis. Scale bar, 300 μ m. *Ab*, electrical activity detected from each of the 64 electrodes from the same slice shown in *a*. *B*, spikes acquired from a single channel were sorted by principal component analysis. Amplitudes of the first three components (PC1, PC2 and PC3) are then displayed in a three-dimensional plot, giving rise to spatially separated clusters, indicative of separate spike waveforms. The four clusters of the three-dimensional plot were obtained with the spike waveforms indicated by the corresponding letters (black line indicates upper and lower spike template limits).



and first peak autocorrelation probability. Their firing frequency histogram showed three smooth distributions with clearly separated peaks (Fig. 2Ba) and significantly different means ($P < 0.001$, unpaired t test; Table 1). In the same way, LRp and LRn-p neurones had distinct autocorrelation probability histogram distributions (Fig. 2Bb) with significantly different means ($P < 0.001$, unpaired t test; Table 1). Accordingly, scatter plots of their basal firing frequency vs. autocorrelation probability and vs. CV (Fig. 2Bc) highlighted a separation into distinct clusters, largely consistent with our heuristic subdivision into three neuronal populations.

Dopamine sensitivity

A very well-known property of the DA neurones of the SNc is their sensitivity to the pharmacological stimulation of D2 autoreceptors, causing membrane hyperpolarisation and reduction in firing frequency (Lacey *et al.* 1987, 1989; Beckstead *et al.* 2004). In order to further characterise the neurones recorded, we focused our attention onto the effect of DA, at a near-maximal concentration ($30 \mu\text{M}$; Lacey *et al.* 1990).

Overall, bath perfusion of $30 \mu\text{M}$ DA (1–2 min) produced an abrupt reduction of firing frequency in the majority of the recorded neurones, often resulting in complete cessation of neuronal firing. The effect of DA reached a steady state within 20–30 s of the onset of drug perfusion and fully recovered after 3–4 min wash. However, as shown in Fig. 3, both the effect of DA and the degree of firing inhibition was not uniform. In fact, some neurones (163/950; 17.16%) did not respond to DA ($\pm 10\%$ change of firing frequency in DA) or even responded with an increase in firing rate ($> 10\%$ change), although only a relatively small number of cells (19/950; 2.00%). With regard to the neurones inhibited by DA, the amount of inhibition was not homogeneous, as suggested by the shoulder in the cumulative distribution of DA effect on firing frequency, at around 60% of the basal rate (Fig. 3A). Thus, some neurones (260/950; 27.37%) were weakly inhibited by DA (firing frequency 60–89% of control in DA), while others (508/950; 53.47%) responded

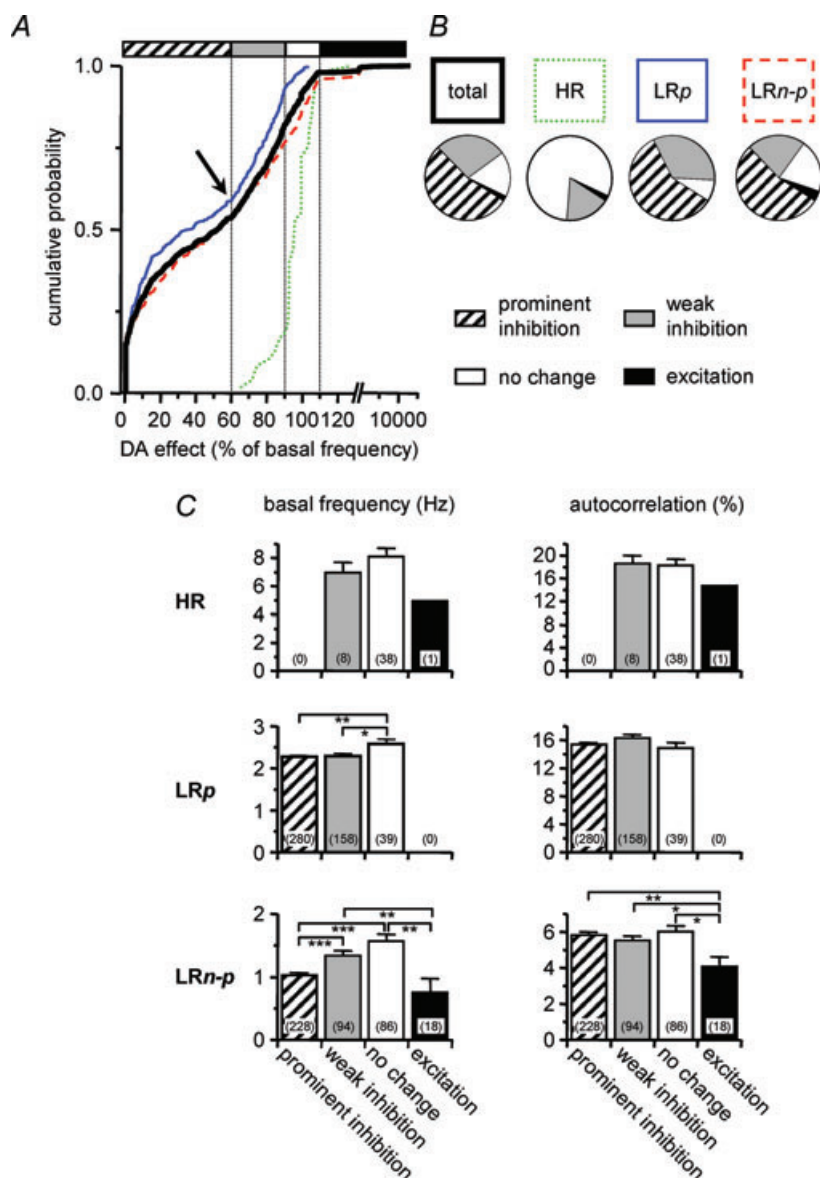
Figure 2. Neuronal classification

A, typical HR (a), LRp (b) and LRn-p (c) neurones. In each panel, the plots on the left are spike time autocorrelograms, while plots on the right are inter-event interval histograms. Horizontal dotted lines in the autocorrelograms indicate 99% confidence limits (Abeles, 1982). Raster plots of spike time stamp are shown on top of each row. B, histograms of the control firing frequency (a) and autocorrelation probability (b) of the three neuronal populations, showing separate relative distributions and distinct peaks. Panels in c are scatter plots of the basal firing rate vs. autocorrelation probability (left) and vs. coefficient of variation (right), showing fairly distinct clusters, corresponding to the three populations.

Table 1. Summary data from high rate (HR), pacemaker low rate (LRp) and non-pacemaker low rate (LRn-p) neurones

	HR (<i>n</i> = 47)	LRp (<i>n</i> = 477)	LRn-p (<i>n</i> = 426)
Basal rate (Hz)	7.85 ± 0.51***	2.27 ± 0.03†††	1.19 ± 0.04§§§
CV	0.49 ± 0.03	0.46 ± 0.01†††	0.72 ± 0.02§§§
Autocorrelation (%)	18.27 ± 0.91**	15.40 ± 0.28†††	5.71 ± 0.13§§§
Number of peaks	6.60 ± 0.66**	14.00 ± 0.73†††	1.35 ± 0.05§§§
Rate in DA (%)	96.20 ± 1.60***	41.13 ± 1.65†	114.85 ± 36.46

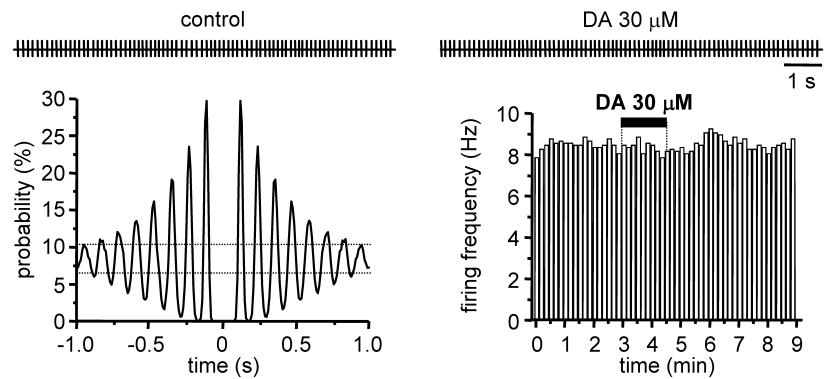
Measurements are shown of the basal firing frequency, coefficient of variation (CV), autocorrelation probability (%) measured from the first peak of the spike time autocorrelograms, the number of symmetric repetitive peaks in the same autocorrelograms exceeding the 99% confidence limit, and the firing rate during perfusion in DA (30 μ M), expressed as percentage of control. The symbols refer to statistical comparisons of HR vs. LRp (*), HR vs. LRn-p (§) and LRp vs. LRn-p (†). The presence of 1, 2 or 3 consecutive symbols stands for $P < 0.05$, $P < 0.01$ and $P < 0.001$, respectively (*t* test for unpaired data).

**Figure 3. Summary of the effect of dopamine on the SNc neurones**

A, cumulative plots of the change in firing frequency mediated by 30 μ M DA, expressed as percentage of control. The thick line is relative to all cells, thin line to LRp cells, dashed line to LRn-p cells and dotted line to HR cells. The effect of DA on the firing rate was separated into prominent inhibition (0–59%; striped box) and weak inhibition (60–89%; grey box), judged by the presence of a shoulder in the rising slope of the cumulative curves, indicated by the black arrow. Additionally, DA effect was defined as no change (90–110%; white box) and excitation (>110%; black box). B, pie plots of the proportion of cells responding with prominent inhibition, weak inhibition, no change or excitation, in all the neurones and in the HR, LRp and LRn-p subpopulations. C, cumulative histograms (mean \pm s.e.m.) of the basal firing rate (left) and autocorrelation probability (right) of the HR (top row), LRp (middle row) and LRn-p (bottom row) neurones, further separated according to their response to 30 μ M DA. The number of cells is indicated in parentheses in each column. Significant differences are shown above the corresponding histograms (* $P < 0.05$; ** $P < 0.01$; *** $P < 0.001$; *t* test for unpaired data).

Figure 4. Dopamine sensitivity of a typical HR neurone

The left panel shows the spike time autocorrelogram of a HR neurone in control conditions. Horizontal dotted lines in the autocorrelogram indicate 99% confidence limits (Abeles, 1982). The plot on the right is a running average histogram of the firing frequency (10 s bins) of the whole experimental session, before, during and after bath perfusion of DA ($30 \mu\text{M}$). Raster plots of spike time stamp are shown on top, during control (left) and DA ($30 \mu\text{M}$) perfusion (right).



to the same treatment with a prominent inhibition (firing frequency 0–59% of control in DA).

When the effect of DA was evaluated in relation to the type of neurone recorded, as defined by the previously

shown classification, we found that the great majority of the HR neurones were DA insensitive ($n = 38$; Fig. 4). Eight HR cells responded with a weak inhibition and one with excitation in $30 \mu\text{M}$ DA, while none of the 47 HR

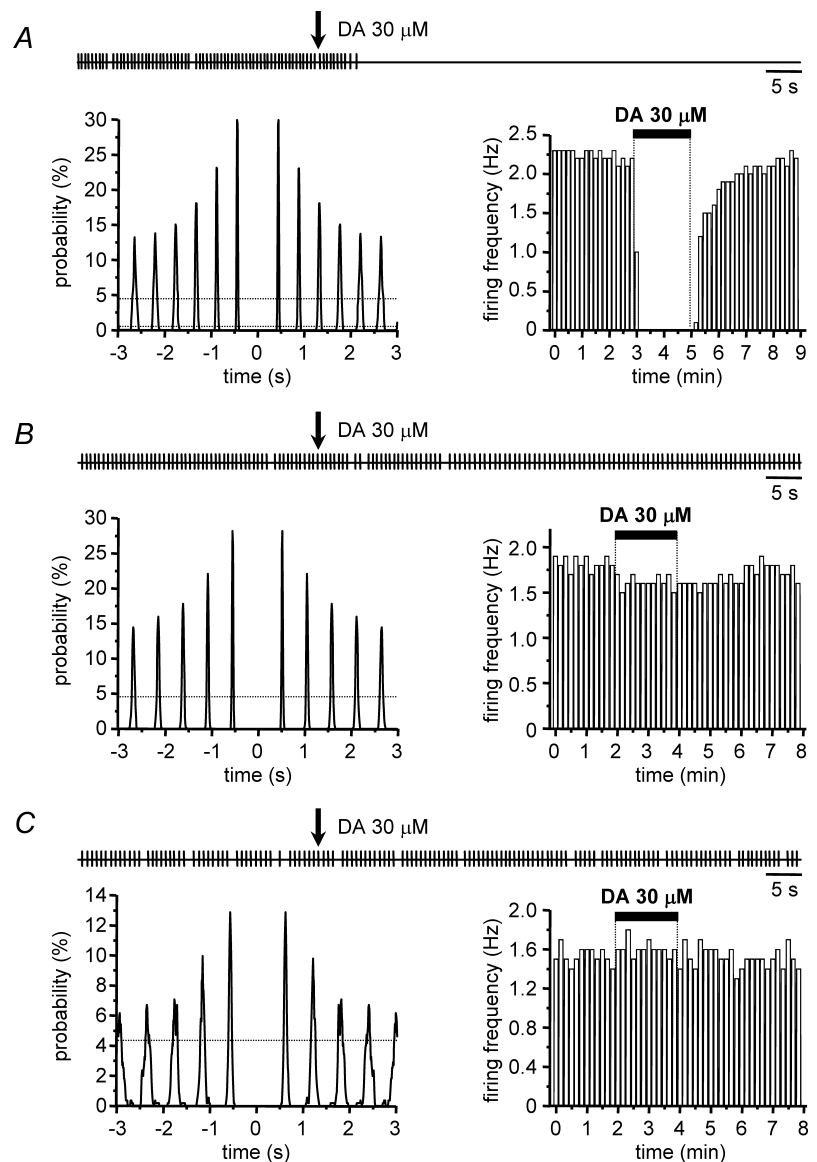


Figure 5. Dopamine sensitivity of LRp neurones

A, B and C are typical LRp neurones responding with prominent inhibition, weak inhibition or no change to DA ($30 \mu\text{M}$), respectively. In each row, left panels are spike time autocorrelograms of the corresponding LRp neurone, in control conditions. Horizontal dotted lines in the autocorrelograms indicate 99% confidence limits (Abeles, 1982). The plots on the right are running average histograms of the firing frequency (10 s bins) of the whole experimental session, before, during and after bath perfusion of DA ($30 \mu\text{M}$). Raster plots of spike time stamp are shown on top, with start of DA ($30 \mu\text{M}$) perfusion indicated by a vertical arrow.

neurons had a prominent inhibition (Fig. 3). Overall, the firing frequency of the HR neurons was $96.20 \pm 1.60\%$ of control in DA (Table 1), suggesting that this category most likely includes typical non-DA, GABAergic neurons of the SNc.

Conversely, LRp neurons were mostly inhibited by $30 \mu\text{M}$ DA (Fig. 3), so that 280 out of the 477 LRp neurons responded to DA with a prominent inhibition of firing frequency, which quickly recovered after DA washout (Fig. 5A), as expected from typical DA neurons of the SNc. However, a significant proportion of these neurons (158/478) were weakly inhibited by DA (Fig. 5B) and it was not unusual to find neurons (39/478) like the one shown in Fig. 5C, with a stable low-rate pacemaker-like firing, typical of a SNc DA neurone, which was unexpectedly insensitive to $30 \mu\text{M}$ DA. Overall, the

firing frequency of the LRp neurons was $41.59 \pm 1.71\%$ of control in DA (Table 1).

The response of the LRn-p neurons to $30 \mu\text{M}$ DA was somewhat less defined, compared to the previous two neuronal populations (Fig. 3), although the majority of the recorded LRn-p cells were still inhibited by DA, either prominently (228/425; Fig. 6A) or weakly (94/425; Fig. 6B). However, the overall firing frequency of the LRn-p neurons in $30 \mu\text{M}$ DA was $114.51 \pm 36.54\%$ of control (Table 1), because a relatively large proportion of these neurons was insensitive to DA (86/425; Fig. 6C) and because of neurons that were excited by DA (17/425). In fact, virtually all of the neurons responding to DA with an increase of firing frequency belonged to the LRn-p category (18/19), hence with a low and irregular basal firing rate, as in the example shown in Fig. 7.

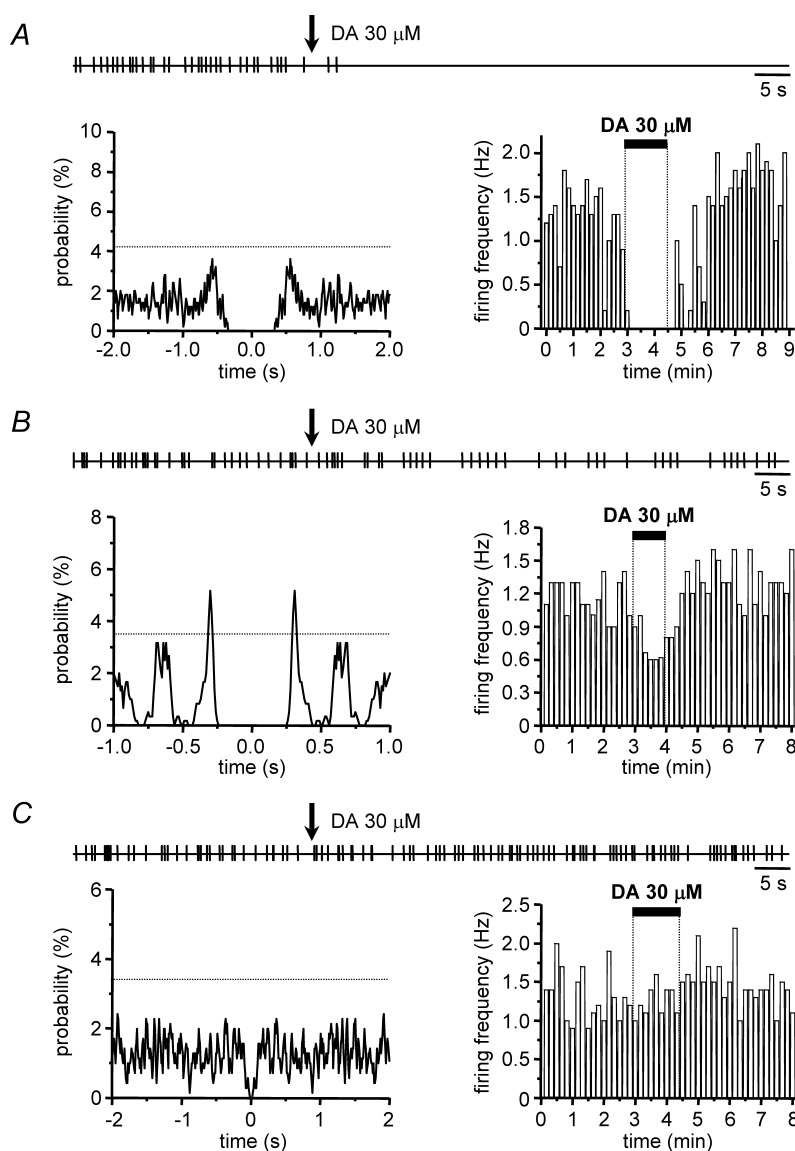


Figure 6. Dopamine sensitivity of LRn-p neurons

A, B and C are typical LRp neurons responding with prominent inhibition, weak inhibition or no change to DA ($30 \mu\text{M}$), respectively. In each row, left panels are spike time autocorrelograms of the corresponding LRn-p neurone, in control conditions. Horizontal dotted lines in the autocorrelograms indicate 99% confidence limits (Abeles, 1982). The plots on the right are running average histograms of the firing frequency (10 s bins) of the whole experimental session, before, during and after bath perfusion of DA ($30 \mu\text{M}$). Raster plots of spike time stamp are shown on top, with start of DA ($30 \mu\text{M}$) perfusion indicated by a vertical arrow.

Investigation of crosscorrelated activity

Following this characterisation, we analysed the firing of each neurone in relation to that of all other neurones in the same slice preparation. Indeed, the relatively high success rate in recording several tens of neurones in the same SNc slice potentially granted us the opportunity to pinpoint crosscorrelated events hardly detectable with other conventional electrophysiological techniques.

One possible source of artefact in this investigation is the theoretical possibility that the firing of one neurone may be simultaneously detected by two separate electrodes, thus providing a false evidence of synchronicity. Indeed, we could find neurones recorded from separate electrodes displaying a high probability of crosscorrelation close to a 0 ms time lag (Fig. 8Ac). However, when we analysed the firing properties of each of the two neurones separately, and we looked at their spike time autocorrelograms throughout the whole time of recording, it became clear that the two neurones were suspiciously behaving as each other's mirror (Fig. 8Aa), i.e. as if they were exactly the same neurone. We could not rule out that these were in fact separate neurones; however, such a highly time-locked synchronised firing has never been described in the SNc. Therefore, we decided to adopt stringent criteria for inclusion of truly synchronised firing by excluding pairs of neurones with constantly matching autocorrelograms, such as those shown in Fig. 8.

Interestingly, this rigorous criterion led us to exclude cases like the one shown in Fig. 8B, with a high probability of synchronised firing for the whole time of recording (Fig. 8Bc) and the two separate autocorrelograms *vs.* time that were virtually identical (Fig. 8Ba), although the two spike waveforms (Fig. 8Bb) suggested that different neurones had been recorded.

Nevertheless, even with these stringent criteria we were able to detect pairs of neurones with a significant number of spikes occurring almost simultaneously. Three examples are shown in Fig. 9. In Fig. 9Aa two clearly different neurones, as indicated by the distinct profile of their spike autocorrelation *vs.* time plot, and by their different sensitivity to DA, had spike crosscorrelation peaks exceeding the 99% confidence limit (Abeles, 1982) around the 0 ms time lag (Fig. 9Ab), indicating the occurrence of synchronised spikes in the two neurones. Altogether, we found 93 neurones displaying a significant degree of firing synchrony with another partner (crosscorrelation peak $2.94 \pm 0.36\%$, in control conditions). Thus, the probability of a cell having a paired neurone in the same slice, weighted by the total number of neurones detected in each slice, was $12.10 \pm 3.14\%$. Most of the crosscorrelated neurones were LR neurones, either weakly (Fig. 9Aa) or prominently (Fig. 9Ac) inhibited by DA. However, we also found DA-insensitive HR neurones ($n = 5$) with a

significant proportion of spikes synchronised with a LR neurone (Fig. 9Ae).

Interestingly, we found indications of the presence of a complex mosaic of crosscorrelated neurones, as indicated by the presence of cells ($n = 13$) having a significant number of spikes synchronised with two other cells, although this never resulted in clusters of synchronised triplets (Fig. 10).

Taking into consideration an interpolar distance of $100 \mu\text{m}$ between the MED64 electrodes, we estimated that the large majority of the paired neurones were $100\text{--}200 \mu\text{m}$ apart, with $300 \mu\text{m}$ as the longest distance observed in one pair.

When we looked at the progression of this synchronised firing during the whole time of recording (Fig. 9B), we noticed a tendency for an increase in crosscorrelation probability associated with DA perfusion, either during drug application (Fig. 9Ba and c), or during drug washout, if spikes had been stopped by DA (Fig. 9Bb). Indeed, when we measured in all synchronised neurones the peak crosscorrelation probability during a 1 min recording in control and in $30 \mu\text{M}$ DA, or as soon as spikes recovered during DA washout, we found a significant increase in firing synchronisation by DA (from 2.94 ± 0.36 to $6.87 \pm 0.79\%$, $P < 0.001$ *t* test for paired data; Fig. 9Bd).

Spatial distribution of the neuronal subpopulations

We took advantage of the MEA technique to try and associate the presence of specific neuronal subpopulations with identified regions of the slice, according to their relative position in the MEA grid. However, we did not find any strong evidence of the preferential distribution of specific neuronal subtypes within the SNc area.

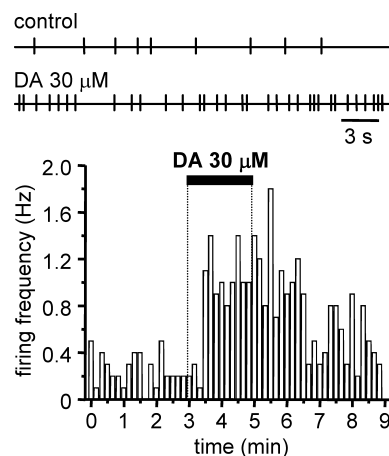


Figure 7. Dopamine-mediated excitation of neuronal firing

The plot is a running average histogram of the firing frequency (10 s bins) of a LRn-p neurone, before, during and after bath perfusion of DA ($30 \mu\text{M}$). Raster plots of spike time stamp are shown above, during control (upper) and DA ($30 \mu\text{M}$) perfusion (lower).

LRp, LRn-p and HR neurones were evenly distributed in the same slice under investigation (Fig. 10B, left panel). Similar results were obtained when neurones were separated based on their DA sensitivity (Fig. 10B, right

panel), or based on the presence of significant cross-correlated firing (Fig. 10B).

This lack of evidence of a specific distribution of the neuronal subpopulations may be due to the horizontal

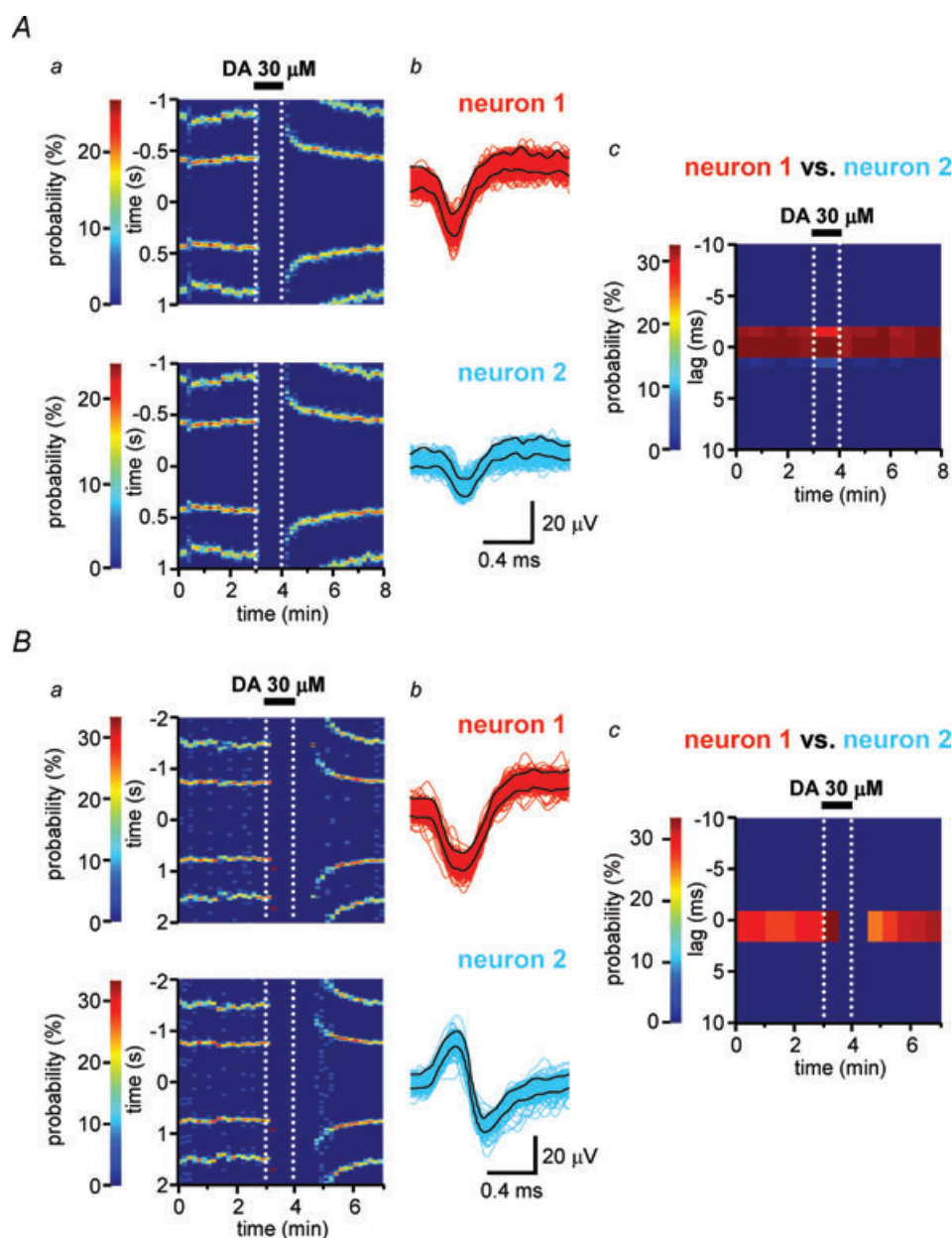


Figure 8. Simultaneous recordings of the same neurone from separate electrodes

Aa and Ba, autocorrelation vs. time plots of spike time stamps recorded by two separate electrodes. Autocorrelation probability is expressed with a colorimetric scale and measured across the whole recording session, at consecutive 10 s intervals. The autocorrelation peaks, measured every 10 s, give rise to continuous horizontal bands over the blue background, reflecting the maintenance of firing regularity. Firing inhibition by DA (30 μM) is expressed by the disappearance of the autocorrelation signal, which slowly recovers at washout. Note the perfect match between the two autocorrelogram vs. time plots, most likely reflecting action potentials of the same neurone, recorded by the two separate electrodes. Spike waveforms detected by the two electrodes are shown in Ab and Bb (black line indicates upper and lower spike template limits). Note the similarity of the two spike waveforms in Ab, as opposed to the different waveforms in Bb. Ac and Bc, crosscorrelation probability expressed with a colorimetric scale and measured across the whole recording session, at consecutive 30 s intervals. Firing synchronicity is shown by the horizontal band around 0 ms.

sectioning angle of the midbrain slices used in our experiments. Therefore, we performed additional control experiments in slices cut along the coronal plane. We recorded a total of 230 neurones from six coronal slices and, in agreement with our previous observations, we could still identify HR, LR*p* and LR*n-p* neurones. Their firing properties and DA sensitivity were analogous to that found in horizontal slices (see Supplemental Fig. 1, available online only). Moreover, we could still highlight the presence of crosscorrelated firing, with a $13.47 \pm 3.62\%$ probability of finding a paired neurone in the same slice.

When we looked at the spatial distribution of the neurones recorded in these coronal slices, we were still unable to find clear evidence of regional clustering of neuronal subtypes, in relation to their firing properties, DA sensitivity or functional connectivity (Supplemental Fig. 2).

Discussion

The present work introduces MEA recordings as a new and powerful technique for the study of the midbrain dopaminergic system *in vitro*. The theoretical advantages of a MEA approach mainly reside in the possibility of recording different types of neurones simultaneously, in controlled *in vitro* experimental conditions. Moreover, neuronal firing is detected using planar extracellular electrodes, free of any direct physical contact with the recorded neurone, thus devoid of the mechanical damage occurring in conventional single-cell recordings and of any interference with the intracellular ionic and molecular content.

An analogous spatio-temporal spike analysis from multiple neurones may also be achieved with functional multi-neurone calcium imaging (Takahashi *et al.* 2007). However, in contrast to this optical recording approach, MEA recordings do not require long-term treatment with membrane-permeable calcium indicators, which interfere with intracellular calcium homeostasis. Moreover, slices from adult animals can be readily used with MEA, without the need to permeate neurones with potentially toxic agents (Takahashi *et al.* 2007). All these advantages suggest that the firing pattern detected using MEA is probably more reliable, although within the limitations inherent in any *in vitro* approach.

Neuronal subpopulations

DA and non-DA midbrain neurones have been distinguished in conventional single-cell extracellular recordings according to the waveform of their action potential (Ungless *et al.* 2004). In our experiments spike waveform was highly variable and could not be associated with selected neuronal populations. In

fact, while single-electrode extracellular recordings allow accurate adjustments of electrode position in order to optimise the neuronal signal, the position of MEA electrodes is fixed. Thus, the proximity of the recording electrode to the site of spike initiation cannot be anticipated. Moreover, both somatic and dendritic spikes can be generated by the DA neurones, with dissimilar shape (Grace & Bunney, 1983*a*; Grace & Onn, 1989; Grace, 1990; Häusser *et al.* 1995; Gentet & Williams, 2007). Indeed, when we compared the spike waveforms of the same neurone detected by two separate electrodes (Fig. 8), we could confirm the unreliability of any characterisation according to spike shape. We thus separated the recorded neurones into three main subpopulations, HR, LR*p* and LR*n-p* neurones, according to their firing properties.

HR neurones, with their higher basal firing rate and overall insensitivity to DA most probably comprise local GABAergic interneurones, described with analogous properties in previous *in vitro* investigations (Lacey *et al.* 1989; Grace & Onn, 1989). The LR*p* and LR*n-p* subpopulations were sorted according to the regularity of their firing, assessed by their spike time autocorrelograms. This criterion follows an analogous method used for the DA neurones of the SNc *in vivo* (Tepper *et al.* 1995; Brazhnik *et al.* 2008). In contrast to these previous studies, we could not find a convincing criterion to distinguish a simply random pattern from a bursting behaviour. However, the lack of a clearly identifiable bursting pattern is not surprising. According to previous investigations, the DA neurones exhibit quite a different firing pattern *in vitro*, compared to *in vivo*, most probably because extrinsic synaptic afferents to the DA neurones are disconnected in a slice preparation. Thus, the bursting pattern of the DA neurones highly expressed in behaving animals is in sharp contrast with the largely regular pattern of the same neurones normally observed *in vitro* (Grace & Onn, 1989).

While a large proportion of all the recorded cells were LR*p* neurones inhibited by DA, resembling the typical DA neurones recorded in the SNc *in vitro* (Lacey *et al.* 1987, 1989; Beckstead *et al.* 2004), a considerable number of LR cells (125/950) were DA insensitive, although the 30 μM concentration used was near-maximal for firing inhibition of the DA neurones (Lacey *et al.* 1989, 1990). Even neurones firing at 2–3 Hz, with a highly regular pacemaker-like pattern, otherwise identified as typical DA neurones, were in fact insensitive to DA ($n = 39$; Figs 3C and 5C). On the other hand, when DA reduced neuronal firing, the degree of inhibition was such that either prominently or weakly inhibited neurones could be identified (Fig. 3). This difference may be ascribed to the different depth of the active neurone from the superficial layer of the slice, directly exposed to the inflow, or to local variation in the efficacy of DA transporters. However, no clear difference was found between prominently or weakly inhibited neurones in the time to reach a steady

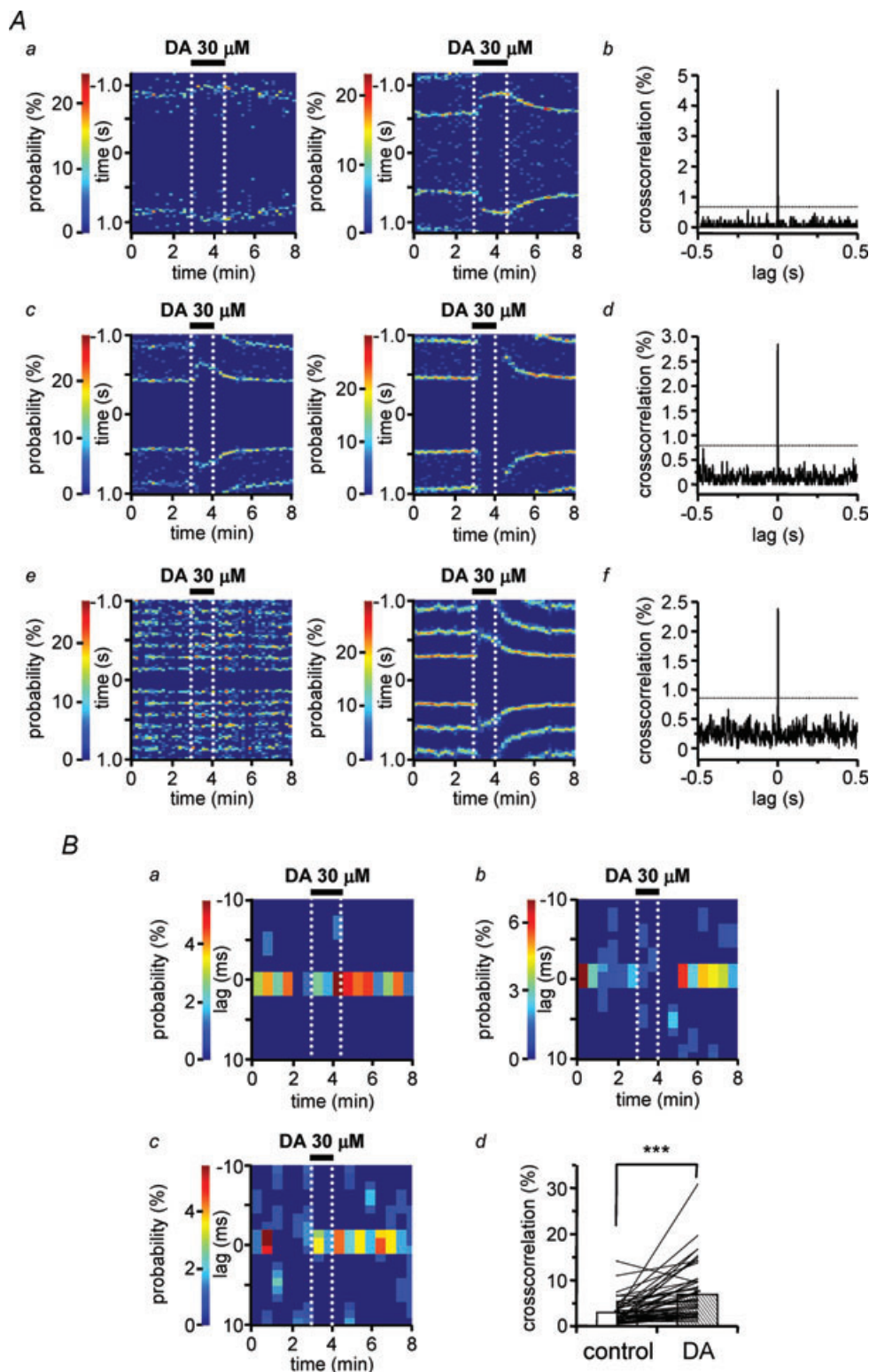


Figure 9. Synchronised firing in distinct SNc neurones

Aa, c and e, autocorrelation vs. time plots of spike time stamps recorded from the same SNc slice, with separate electrodes. Autocorrelation probability is expressed with a colorimetric scale and measured across the whole recording session, at consecutive 10 s intervals. The autocorrelation peaks, measured every 10 s, give rise to continuous horizontal bands over the blue background, reflecting the maintenance of firing regularity. DA (30 μM) effect on neuronal firing is expressed in Aa, c and e (right panel) by the shift or disappearance of the autocorrelation signal, which slowly recovers at washout, while no effect of DA was evident in Ae (left panel). The panels in Ab, d

state of firing inhibition, or firing recovery at washout, as expected if this difference depended on DA reuptake or drug diffusion across the tissue.

Instead, the dissimilar sensitivity to DA seems to be indicative of specific neuronal subpopulations. This hypothesis is sustained by our comparative analysis of the firing properties of the neurones sorted according to their DA sensitivity. Thus, among the LRP neurones, significant differences were found in the basal firing rate of DA-inhibited vs. DA-insensitive cells (Fig. 3C). Similarly, significant differences were found in the firing rate of LRn-p neurones, depending on their response to DA (Fig. 3C).

This distinction according to DA sensitivity may be due to different D2 autoreceptor responses; however, it may also be a secondary effect of differences in their basal firing rate. As reported by Putzier *et al.* (2009), DA neurones become progressively less susceptible to firing inhibition by pharmacological agents as their basal firing rate increases.

Independently of the underlying mechanisms, it seems evident that the use of a MEA approach provides a much more complex picture with regard to firing pattern and DA sensitivity of the SNc neurones, compared to previous investigations. We cannot say whether this difference is due to our recording approach, which leaves recorded neurones in a more near-physiological condition, or whether conventional single-cell techniques are intrinsically biased towards a specific cell type, more easily accessed by the glass electrode. Alternatively, the variability that we observed may be ascribed to contamination from nearby VTA or substantia nigra pars reticulata neurones. Indeed, electrodes close to the medial side might have detected firing from the VTA, but this contamination was limited by our care not to place MEA electrodes beyond the MT, on the medial side of the slice. Moreover, when we tried to map neuronal subpopulations in relation to their position in the slice, we found that regular and irregular neurones were evenly distributed in the slice, with no evidence of specific clustering close to the medial area, indicative of VTA contamination. We have also shown that similar results, in terms of firing properties and DA sensitivity, could be observed in SNc neurones recorded from coronal midbrain slices, thus ruling out that this

variability might be ascribed to a different degree of dendritic truncation during the slicing procedure (Lin *et al.* 2003).

The concept of a separation between DA and non-DA neurones simply based on their membranes properties and postsynaptic hyperpolarisation through D2 autoreceptor stimulation has been challenged by recent investigations in the VTA. Single-unit recordings in the VTA *in vivo* have shown similar basal firing rates of DA and non-DA neurones (Ungless *et al.* 2004). Moreover, *in vitro* experiments in the VTA have shown that the presence of a prominent I_h is not peculiar to tyrosine hydroxylase-positive neurones, nor their sensitivity to D2 autoreceptor stimulation (Margolis *et al.* 2006), while distinctions among the VTA neurones seem to correlate with their relative area of projection (Lammel *et al.* 2008; Margolis *et al.* 2008).

With regard to the SNc, the functional and molecular diversity among the DA neurones is a much debated topic (Liss & Roeper, 2008). These neurones appear to be involved in a wide variety of functions, including motor control and reward-based learning (Björklund & Dunnett, 2007; Schultz, 2007; Wise, 2009). Indeed, a recent report in the monkey has demonstrated different responses to rewarding or aversive stimuli of SNc DA neurones, although no significant differences were found in their firing properties (Matsumoto & Hikosaka, 2009). Moreover, the differential vulnerability to degeneration observed within the DA neuronal population of the SNc in Parkinson's disease (Damier *et al.* 1999) is another indicator of a non-homogeneous population.

In a small number of neurones we found excitation induced by 30 μ M DA. These neurones were basically all characterised by a low (<1 Hz) and highly irregular basal activity, compared to other cell groups. The nature of this excitation needs further investigation, with experiments focused on the identification of the DA receptor involved and demonstrating a direct effect on the postsynaptic neurone.

Synchronous firing in the SNc

It is a widely accepted concept that basal ganglia function is not a simple expression of the sum of

and f are crosscorrelation probability plots obtained from the corresponding pairs on the left, measured from the whole recording time (1 ms bin size). Horizontal dotted lines in the crosscorrelograms indicate 99% confidence limits (Abeles, 1982). *Ba*, *b* and *c*, crosscorrelation probability expressed with a colorimetric scale and measured across the whole recording session, at consecutive 30 s intervals, refers to the pairs of neurones shown in *Aa*, *c* and *e*, respectively. Firing synchronicity is shown by the horizontal band around 0 ms. Note the increase in crosscorrelation probability associated with DA (30 μ M) during drug perfusion (*a* and *c*) or when spikes recovered at drug washout (*b*). *Bd*, superimposed histogram (mean \pm S.E.M.) and scatter plot of the crosscorrelation probability measured from all pairs of neurones ($n = 53$) during 1 min recording in control conditions and in DA, or when firing inhibition started to recover. The two populations were significantly different ($***P < 0.001$; t test for paired data).

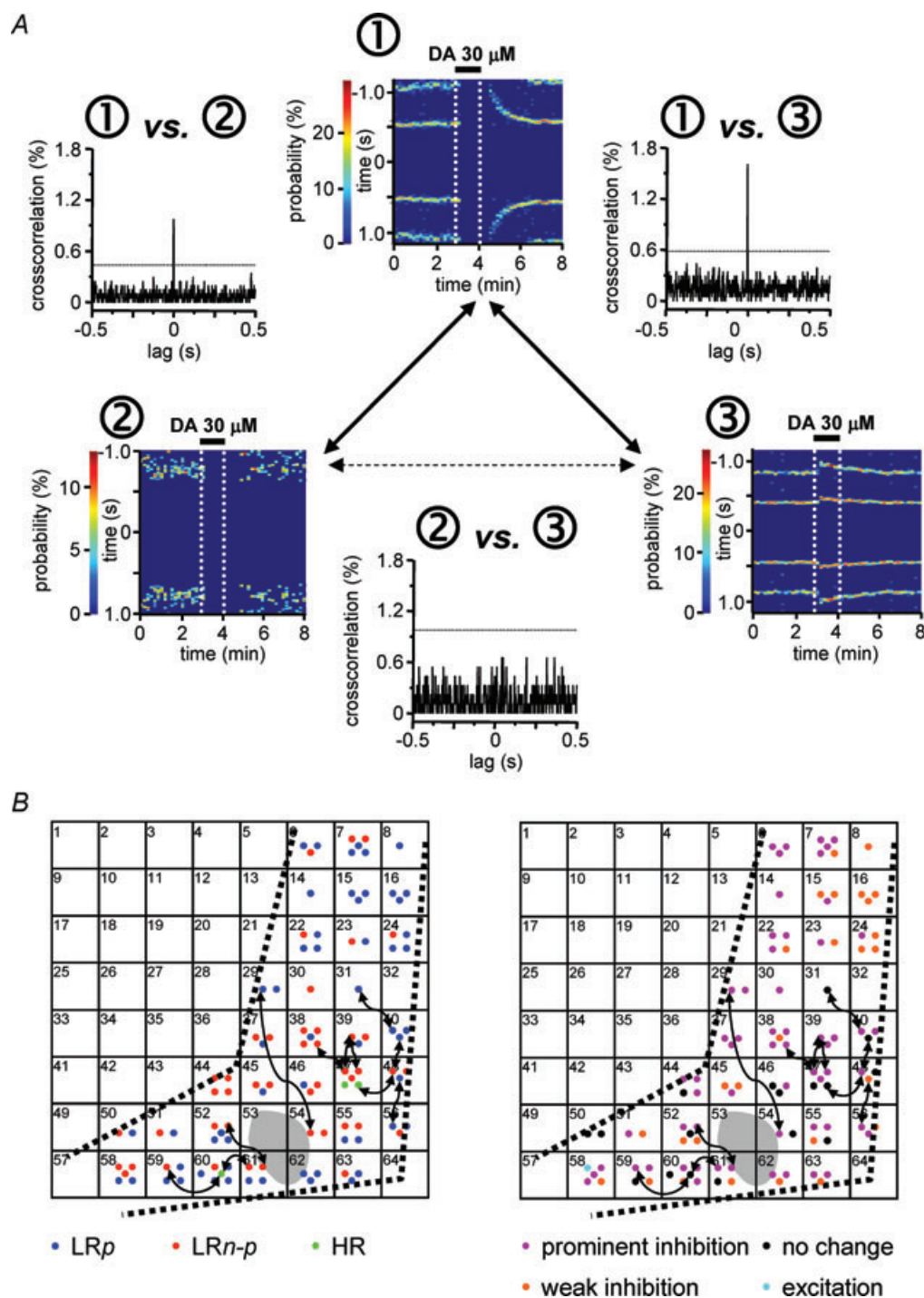


Figure 10. Multiple pairings of synchronised firing in SNc neurones

A, autocorrelation vs. time plots of spike time stamps recorded from the same SNc slice with separate electrodes of neurone 1, neurone 2 and neurone 3. The different profiles of autocorrelation probability and sensitivity to $30\ \mu\text{M}$ DA clearly show that they are different neurones. Crosscorrelation probability plots obtained from the corresponding pairs indicated the occurrence of synchronised firing in 1 vs. 2 and in 1 vs. 3, but not in 2 vs. 3. Crosscorrelograms were measured from the whole recording time (1 ms bin size). Horizontal dotted lines in the crosscorrelograms indicate 99% confidence limits (Abeles, 1982). **B**, mapping of the neuronal distribution in the same horizontal slice, in relation to their corresponding position in the 64 channels MEA grid. The grey area indicates MT position, while the two black dotted lines define the borders of the crescent-like SNc area. Neurones are colour-coded according to their classification into HR, LRp and LRn-p neurones (left panel) or sensitivity to DA ($30\ \mu\text{M}$), as prominent inhibition, weak inhibition, no change or excitation (right panel). Black double-headed lines are used to link neurones functionally connected by a significant proportion of crosscorrelated spikes.

individual excitatory/inhibitory connections between separate neurones of its nuclei. Indeed, specific firing patterns of oscillatory activity in synchronised neuronal populations encode information during both physiological and pathological conditions (Wichmann & DeLong, 1996; Gatev *et al.* 2006; Hammond *et al.* 2007). With regard to the SNc, the occurrence of synchronised firing was first reported in the rat *in vivo* by Grace & Bunney (1983b), and more recently confirmed in the monkey (Morris *et al.* 2004; Joshua *et al.* 2009). The simultaneous recording of a high number of units with our MEA approach granted us the unique possibility of gaining new insights into the collective firing of the SNc neurones in *in vitro* experimental conditions. Using this approach, we found SNc neurones with a significant proportion of spikes occurring synchronously, with a $12.10 \pm 3.14\%$ probability of finding paired neurones in each slice. This value is smaller than the 27% probability reported *in vivo* by Morris *et al.* (2004), probably because of the limited three-dimensional extension of the neuronal network in a slice preparation.

The mechanism underlying firing synchronisation needs further investigation. Electrotonic coupling has been reported by Grace & Bunney (1983b), and recently confirmed *in vitro* (Vandecasteele *et al.* 2005, 2008; but see Lin *et al.* 2003), although the low-pass filtering properties of local electrical synapses seem to hardly sustain action potential synchronisation (Vandecasteele *et al.* 2005). Alternatively, common inhibitory inputs to the SNc (Tepper & Lee, 2007) may enable a significant proportion of spikes from separate neurones to be entrained by a common synaptic hyperpolarisation (Cobb *et al.* 1995), alone or in combination with electrotonic couplings (Pfeuty *et al.* 2007).

It has been proposed that synchronisation of the DA neurones may have an important physiological significance in enhancing the overall DA signalling into target areas (Joshua *et al.* 2009); however, the low number of neurones simultaneously recorded *in vivo* does not allow an accurate description of the extent of cellular synchronisation. Using a MEA *in vitro* approach, we could confirm the presence of a probably more complex network of synchronised neurones, not limited to just separate pairs. Moreover, neuronal synchronisation was expressed among presumed DA neurones, but it was unlikely to be limited to this neuronal population. The presence of such functionally connected neurones could give rise to local clusters of paired neurones, although we found no strong evidence of specific subregions of the SNc where paired neurones were preferentially located, either in horizontal (Fig. 10B) or coronal (Supplemental Fig. 2) slices.

In control conditions, the degree of firing synchronisation, though statistically significant, was small ($\sim 2\%$), casting doubts on its physiological role. However, we found that DA perfusion was associated

with a significant increase in crosscorrelation probability (to $\sim 7\%$), suggesting a more dynamic and functionally relevant phenomenon. Interestingly, an increase in synchronisation of DA neurones has been reported *in vivo* in monkeys exposed to rewarding stimuli, during a classical conditioning task (Joshua *et al.* 2009). It is tempting to speculate that the increase in DA neurone firing during a rewarding task causes DA release in the SNc, responsible for local neuronal synchronisation. Indeed, DA neurones are activated by rewarding stimuli and are thought to encode reinforcement of reward-based learning (Schultz, 1997; Hollerman & Schultz, 1998; Morris *et al.* 2006; Cohen & Frank, 2009). However, Joshua *et al.* (2009) showed that both rewarding and aversive stimuli cause an increase in DA neurone firing, while rewarding stimuli only are associated with enhanced synchronisation.

Concluding remarks

Single-unit MEA recordings in slices of the ventral midbrain reveal a high degree of complexity in the classification of the SNc neurones and open new perspectives in the scientific investigation of the dopaminergic system *in vitro*. The advantages of this experimental approach do not simply reside in the high number of neurones that can be recorded during a single experimental session, but more importantly in the possibility of investigating the functional connectivity and network properties of the SNc neurones. This may reveal new cellular and molecular mechanisms underlying the dopaminergic neurotransmission and propose new targets for the pharmacological treatment of DA-dependent neurological disorders.

References

- Abeles M (1982). Quantification, smoothing, and confidence limits for single-units' histograms. *J Neurosci Methods* **5**, 317–325.
- Beckstead MJ, Grandy DK, Wickman K & Williams JT (2004). Vesicular dopamine release elicits an inhibitory postsynaptic current in midbrain dopamine neurons. *Neuron* **42**, 939–946.
- Björklund A & Dunnett SB (2007). Dopamine neuron systems in the brain: an update. *Trends Neurosci* **30**, 194–202.
- Brazhnik E, Shah F & Tepper JM (2008). GABAergic afferents activate both GABA_A and GABA_B receptors in mouse substantia nigra dopaminergic neurons *in vivo*. *J Neurosci* **28**, 10386–10398.
- Cobb SR, Buhl EH, Halasy K, Paulsen O & Somogyi P (1995). Synchronization of neuronal activity in hippocampus by individual GABAergic interneurons. *Nature* **378**, 75–78.
- Cohen MX & Frank MJ (2009). Neurocomputational models of basal ganglia function in learning, memory and choice. *Behav Brain Res* **199**, 141–156.

- Damier P, Hirsch EC, Agid Y & Graybiel AM (1999). The substantia nigra of the human brain: II. Patterns of loss of dopamine-containing neurons in Parkinson's disease. *Brain* **122**, 1437–1448.
- Egert U, Heck D & Aertsen A (2002). Two-dimensional monitoring of spiking networks in acute brain slices. *Exp Brain Res* **142**, 268–274.
- Egert U, Schlosshauer B, Fennrich S, Nisch W, Fejtli M, Knott T, Müller T & Hämmeler H (1998). A novel organotypic long-term culture of the rat hippocampus on substrate-integrated multielectrode arrays. *Brain Res Brain Res Protoc* **2**, 229–242.
- Gatev P, Darbin O & Wichmann T (2006). Oscillations in the basal ganglia under normal conditions and in movement disorders. *Mov Disord* **21**, 1566–1577.
- Gentet LJ & Williams SR (2007). Dopamine gates action potential backpropagation in midbrain dopaminergic neurons. *J Neurosci* **27**, 1892–1901.
- Geracitano R, Tozzi A, Berretta N, Florenzano F, Guatteo E, Viscomi MT, Chiolo B, Molinari M, Bernardi G & Mercuri NB (2005). Protective role of hydrogen peroxide in oxygen-deprived dopaminergic neurones of the rat substantia nigra. *J Physiol* **568**, 97–110.
- Giustizieri M, Cucchiaroni ML, Guatteo E, Bernardi G, Mercuri NB & Berretta N (2007). Memantine inhibits ATP-dependent K⁺ conductances in dopamine neurons of the rat substantia nigra pars compacta. *J Pharmacol Exp Ther* **322**, 721–729.
- Grace AA (1990). Evidence for the functional compartmentalization of spike generating regions of rat midbrain dopamine neurons recorded in vitro. *Brain Res* **524**, 31–41.
- Grace AA & Bunney BS (1983a). Intracellular and extracellular electrophysiology of nigral dopaminergic neurons–2. Action potential generating mechanisms and morphological correlates. *Neuroscience* **10**, 317–331.
- Grace AA & Bunney BS (1983b). Intracellular and extracellular electrophysiology of nigral dopaminergic neurons–3. Evidence for electrotonic coupling. *Neuroscience* **10**, 333–348.
- Grace AA & Onn SP (1989). Morphology and electrophysiological properties of immunocytochemically identified rat dopamine neurons recorded in vitro. *J Neurosci* **9**, 3463–3481.
- Hammond C, Bergman H & Brown P (2007). Pathological synchronization in Parkinson's disease: networks, models and treatments. *Trends Neurosci* **30**, 357–364.
- Häusser M, Stuart G, Racca C & Sakmann B (1995). Axonal initiation and active dendritic propagation of action potentials in substantia nigra neurons. *Neuron* **15**, 637–647.
- Hollerman JR & Schultz W (1998). Dopamine neurons report an error in the temporal prediction of reward during learning. *Nat Neurosci* **1**, 304–309.
- Jia Y, Nguyen T, Desai M & Ross MG (2008). Programmed alterations in hypothalamic neuronal orexigenic responses to ghrelin following gestational nutrient restriction. *Reprod Sci* **15**, 702–709.
- Joshua M, Adler A, Prut Y, Vaadia E, Wickens JR & Bergman H (2009). Synchronization of midbrain dopaminergic neurons is enhanced by rewarding events. *Neuron* **62**, 695–704.
- Kent J & Meredith AL (2008). BK channels regulate spontaneous action potential rhythmicity in the suprachiasmatic nucleus. *PLoS One* **3**, e3884.
- Lacey MG, Mercuri NB & North RA (1987). Dopamine acts on D₂ receptors to increase potassium conductance in neurones of the rat substantia nigra zona compacta. *J Physiol* **392**, 397–416.
- Lacey MG, Mercuri NB & North RA (1989). Two cell types in rat substantia nigra zona compacta distinguished by membrane properties and the actions of dopamine and opioids. *J Neurosci* **9**, 1233–1241.
- Lacey MG, Mercuri NB & North RA (1990). Actions of cocaine on rat dopaminergic neurones in vitro. *Br J Pharmacol* **99**, 731–735.
- Lammel S, Hetzel A, Häckel O, Jones I, Liss B & Roeper J (2008). Unique properties of mesoprefrontal neurons within a dual mesocorticolimbic dopamine system. *Neuron* **57**, 760–773.
- Lin JY, van Wyk M, Bowala TK, Teo MY & Lipski J (2003). Dendritic projections and dye-coupling in dopaminergic neurons of the substantia nigra examined in horizontal brain slices from young rats. *J Neurophysiol* **90**, 2531–2535.
- Liss B & Roeper J (2008). Individual dopamine midbrain neurons: functional diversity and flexibility in health and disease. *Brain Res Rev* **58**, 314–321.
- Mann EO, Suckling JM, Hajos N, Greenfield SA & Paulsen O (2005). Perisomatic feedback inhibition underlies cholinergically induced fast network oscillations in the rat hippocampus in vitro. *Neuron* **45**, 105–117.
- Mapelli J & D'Angelo E (2007). The spatial organization of long-term synaptic plasticity at the input stage of cerebellum. *J Neurosci* **27**, 1285–1296.
- Margolis EB, Lock H, Hjelmstad GO & Fields HL (2006). The ventral tegmental area revisited: is there an electrophysiological marker for dopaminergic neurons? *J Physiol* **577**, 907–924.
- Margolis EB, Mitchell JM, Ishikawa J, Hjelmstad GO & Fields HL (2008). Midbrain dopamine neurons: projection target determines action potential duration and dopamine D₂ receptor inhibition. *J Neurosci* **28**, 8908–8913.
- Matsumoto M & Hikosaka O (2009). Two types of dopamine neuron distinctly convey positive and negative motivational signals. *Nature* **459**, 837–841.
- Mercuri NB, Bonci A, Calabresi P, Stefani A & Bernardi G (1995). Properties of the hyperpolarization-activated cation current I_h in rat midbrain dopaminergic neurons. *Eur J Neurosci* **7**, 462–469.
- Morris G, Arkadir D, Nevet A, Vaadia E & Bergman H (2004). Coincident but distinct messages of midbrain dopamine and striatal tonically active neurons. *Neuron* **43**, 133–143.
- Morris G, Nevet A, Arkadir D, Vaadia E & Bergman H (2006). Midbrain dopamine neurons encode decisions for future action. *Nat Neurosci* **9**, 1057–1063.
- Oka H, Shimono K, Ogawa R, Sugihara H & Taketani M (1999). A new planar multielectrode array for extracellular recording: application to hippocampal acute slice. *J Neurosci Methods* **93**, 61–67.
- Paxinos G & Watson C (1986). *The Rat Brain in Stereotaxic Coordinates*. Academic Press Australia, North Ryde.

- Pfeuty B, Golomb D, Mato G & Hansel D (2007). Inhibition potentiates the synchronizing action of electrical synapses. *Front Comput Neurosci* **1**, 8.
- Putzier I, Kullmann PHM, Horn JP & Levitan ES (2009). Dopamine neuron responses depend exponentially on pacemaker interval. *J Neurophysiol* **101**, 926–933.
- Schultz W (1997). Dopamine neurons and their role in reward mechanisms. *Curr Opin Neurobiol* **7**, 191–197.
- Schultz W (2007). Multiple dopamine functions at different time courses. *Annu Rev Neurosci* **30**, 259–288.
- Stett A, Egert U, Guenther E, Hofmann F, Meyer T, Nisch W & Haemmerle H (2003). Biological application of microelectrode arrays in drug discovery and basic research. *Anal Bioanal Chem* **377**, 486–495.
- Takahashi N, Sasaki T, Usami A, Matsuki N & Ikegaya Y (2007). Watching neuronal circuit dynamics through functional multineuron calcium imaging (fMCI). *Neurosci Res* **58**, 219–225.
- Tepper JM & Lee CR (2007). GABAergic control of substantia nigra dopaminergic neurons. *Prog Brain Res* **160**, 189–208.
- Tepper JM, Martin LP & Anderson DR (1995). GABA_A receptor-mediated inhibition of rat substantia nigra dopaminergic neurons by pars reticulata projection neurons. *J Neurosci* **15**, 3092–3103.
- Ungless MA, Magill PJ & Bolam JP (2004). Uniform inhibition of dopamine neurons in the ventral tegmental area by aversive stimuli. *Science* **303**, 2040–2042.
- van Aerde KI, Heistek TS & Mansvelder HD (2008). Prelimbic and infralimbic prefrontal cortex interact during fast network oscillations. *PLoS One* **3**, e2725.
- Vandecasteele M, Glowinski J, Deniau JM & Venance L (2008). Chemical transmission between dopaminergic neuron pairs. *Proc Natl Acad Sci U S A* **105**, 4904–4909.
- Vandecasteele M, Glowinski J & Venance L (2005). Electrical synapses between dopaminergic neurons of the substantia nigra pars compacta. *J Neurosci* **25**, 291–298.
- Whitson J, Kubota D, Shimono K, Jia Y & Taketani M (2006). Multi-electrode arrays: enhancing traditional methods and enabling network physiology. In *Advances in Network Electrophysiology – Using Multi-electrode Arrays*, ed. Taketani M & Baudry M, pp. 38–68. Springer, Singapore.
- Wichmann T & DeLong MR (1996). Functional and pathophysiological models of the basal ganglia. *Curr Opin Neurobiol* **6**, 751–758.
- Wise RA (2009). Roles for nigrostriatal—not just mesocorticolimbic—dopamine in reward and addiction. *Trends Neurosci* **32**, 517–524.

Author contributions

All experiments were conducted in the laboratories of Experimental Neurology at the Fondazione Santa Lucia IRCCS in Rome, Italy. N.B. collected, analysed and interpreted the data, as well as drafting the manuscript. N.B. and N.B.M. conceived and designed the experiments. N.B.M. and G.B. revised the article for important intellectual content. All authors approved the final version of the manuscript.

Acknowledgements

We are deeply grateful to Professor J. Lipski (University of Auckland, NZ) for critically reading the manuscript and to Dr A. Paziienti (EBRI Foundation, Rome, Italy) for his helpful advice in data analysis. This work was supported by a grant PS05.15M from Ministero della Salute.